Characterizing human retinotopic mapping with conformal geometry: A preliminary study

Duyan Ta[a], Jie Shi[a], Brian Barton[b], Alyssa Brewer[b], Zhong-Lin Lu[c], Yalin Wang[a]

[a]Arizona State University, Ira A. Fulton School of Computing, Informatics, and Decision Systems Engineering, Tempe, AZ, USA 85281;

[b]University of California Irvine, Irvine, CA, USA 92697;

[c]The Ohio State University, 1835 Neil Avenue, Columbus, OH, USA 43210

ABSTRACT

Functional magnetic resonance imaging (fMRI) has been widely used to measure the retinotopic organization of early visual cortex in the human brain. Previous studies have identified multiple visual field maps (VFMs) based on statistical analysis of fMRI signals, but the resulting geometry has not been fully characterized with mathematical models. Here we test whether VFMs V1 and V2 obey the least restrictive of all geometric mappings; that is, whether they are angle-preserving and therefore maintain conformal mapping. We measured retinotopic organization in individual subjects using standard traveling-wave fMRI methods. Visual stimuli consisted of black and white, drifting checkerboards comprising rotating wedges and expanding rings to measure the cortical representations of polar angle and eccentricity, respectively. These representations were then projected onto a 3D cortical mesh of each hemisphere. By generating a mapped unit disk that is conformal of the VFMs using spherical stereographic projection and computing the parameterized coordinates of the eccentricity and polar angle gradients, we computed Beltrami coefficients to check whether the mapping from the visual field to the V1 and V2 cortical representations is conformal. We find that V1 and V2 exhibit local conformality. Our analysis of the Beltrami coefficient shows that selected regions of V1 and V2 that contain reasonably smooth eccentricity and polar angle gradients do show significant local conformality, warranting further investigation of this approach for analysis of early and higher visual cortex. These results suggest that such a mathematical model can be used to characterize the early VFMs in human visual cortex.

Keywords: retinotopic mapping, conformal geometry, Beltrami coefficient, functional magnetic resonance imaging, visual field maps,

1. INTRODUCTION

The efficiency of the measurements and the relatively large amplitude of functional magnetic resonance imaging (fMRI) signals in visual cortical areas have made it possible to develop quantitative models of functional responses within specific maps in individual subjects. Retinotopic mapping of human visual cortex generates visual field maps by analyzing stimulus-referred fMRI response to each of the fragments in each voxel.[9,6,16,8,10,18] The maps elucidate the spatial organization of the neuronal responses to visual images on the retina[6,9,8,13,16,17] and have contributed greatly to our understanding of the human visual system and the development of human cerebral cortex. They also hold great promises to further our understanding of plasticity in the human visual cortex and thus improve the rehabilitation efficacy on various patients with visual function loss. Numerous studies have been devoted to retinotopic mapping and they have helped us to understand the human cortical structure and early vision process. Previous studies have identified multiple visual field maps (VFMs) based on statistical analysis of fMRI signals, but the resulting geometry has not been fully characterized with mathematical models. This paper explores using conformal surface parameterization and the Beltrami coefficient on measured retinotopic organization data using standard traveling-wave fMRI methods to understand if they can be used to fully characterize the early visual field maps.

1.1 Related work

Retinotopic mapping of human visual cortex, based on functional magnetic resonance imaging (fMRI), was investigated to understand the spatial organization of the neuronal responses to visual images on the retina.[6,8,9,13,16,17] Typical retinotopy is carried out in three main steps: (1) Use structural scans to flatten the cortical surfaces; (2) Project collected functional data onto the flattened cortical surfaces; (3) Generate a phase map of the retina image on the flattened surface based on the visual stimuli on the retina. The current approach has issues with large distortions that are usually generated in the cortical flattening process and the lack of a concrete mathematical description to compare the generated maps. These maps are mainly described by analyzing individual images and there is no concrete mathematical description to compare these maps. These limitations have made retinotopic mapping mainly an experimental study that differs from experiment to experiment. Experimental results are mainly confined to only small group collected sample population data. In order to fully do a population level integration and analysis of the retinotopic maps, there needs to be a mathematical model that can fully describe these maps.

Recent developments in brain imaging have accelerated the collection of both high resolution fMRI and MRI data. It has allowed researchers to study the visual and auditory processing capabilities of the brain in greater detail than ever before.[3,4,5,19] The early visual processing system of the brain has been investigated extensively but only recently has it been possible to study them in the depth and detail that is making it possible to look at similarities and differences across a large population sample set.[4,5,19] In 2006, Qiu et. al.[12] used the circle packing method to conformally flatten V1 to a hyperbolic disk for visualization of precisely measured retinotopic data but did not go further and propose a mathematical model. More recently in 2010, Balasubramanian and Schwartz[2] have found that the organization of the visual areas of the brain is much more alike across subjects than previously expected when isometric flattening is applied on all the brain surfaces. Over years, there are accumulated evidences that support a long-term hypothesis: the retinotopic mapping is a conformal mapping.[7,14] The early complex-log transform model proposed by Schwartz[14] is the most well-known expression for describing the human V1 because it is straightforward and simple. There have been improvements and variations to the Schwartz[14] model over the years as better experimental data gradually became available. However, the conformal mapping hypothesis remains unproven. The validation of this hypothesis in some form will not only enrich our understanding in cognitive science but it will also help develop efficient therapies for visual dysfunctions.

1.2 Overview

We measured retinotopic organization in individual subjects using standard traveling-wave fMRI methods. Visual stimuli consisted of black and white, drifting checkerboards comprising rotating wedges and expanding rings to measure the cortical representations of polar angle and eccentricity, respectively. These representations were then projected onto a 3D cortical mesh of each hemisphere.[4,5,19] Figure 1 shows the standard traveling-wave fMRI data and the color coded activated visual areas on a flattened cortical surface. The eccentricity data collection is shown on the left panel and the polar angle data is shown on the right panel.

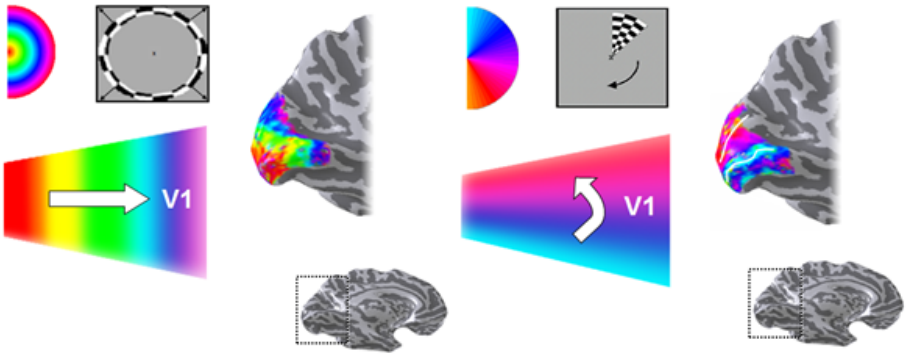

Figure 1. Standard traveling-wave fMRI data. Eccentricity data collection is on the left and polar angle data collection is on the right.

To verify if the retinotopic map is a conformal map, we take a two-step approach. First, we will compute a conformal mapping from the brain visual cortical surface to a unit disk. Second, we establish a mapping from the visual field to the unit disk. Let S_r, S_v, S_d denote visual field, visual surface, and the unit disk, respectively. We further assume the

mapping functions between them are $f: S_r \to S_v, g: S_v \to S_d, h = g \circ f: S_r \to S_d$. We compute the mapping function, g, with our brain surface conformal mapping method. Given g is a conformal mapping, our logic is that by checking if function h is conformal, we will be able to check if f is conformal

Figure 2. illustrates how we compute the conformal mapping from the brain visual area to the unit disk. Fig. 2 (a) shows a left cortical hemisphere overlaid with pseudo-color of responses to eccentricity stimuli; (b) a visual surface patch cut along the plane shown in (a), (c) a closed genus zero surface that is generated by a double covering of surface patch in (b), i.e. for any face $[v_i, v_j, v_k]$, we can generate a new face $[\bar{v}_i, \bar{v}_k, \bar{v}_j]$ that is geometrically identical to the original face but with opposite normal direction. A nonlinear heat diffusion based spherical conformal parameterization method[21] is applied to compute a conformal mapping from the double covering surface to a sphere (d). Finally, by a stereographic projection of the hemisphere to the complex plane, we achieve the conformal mapping from a visual cortical surface to the unit disk on the complex plane (e).

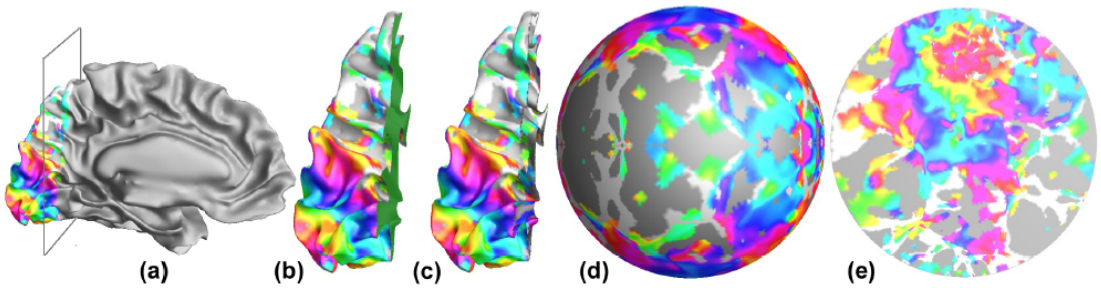

Figure 2. Conformal mapping to unit disk of visual regions cut from cortical mesh. In (a), we slice along a plane to separate the visual regions from the rest of the cortical mesh. (b) is the resulting open mesh containing only the visual regions after slicing. (c) is the double covering of the open mesh. (d) is the projection of the double covered mesh to a sphere. (e) is the the stereographic projection of the conformal sphere to a unit disk.

By using the position encoded gradient color data that was embedded onto the cortical mesh vertices during the traveling-wave data collection phase, we can compute the location of the visual stimulus in the visual field when given a vertex in the visual area simply as u = rcos(θ) and v = rsin(θ). The value of r comes from the eccentricity color data while the value of θ comes from polar angle color data. Figure 3 shows the steps for retrieving the parameterized uv coordinates of a selected region. (a) shows the what a flattened V1 visual area looks like with eccentricity color data projected onto the cortical mesh after processing of the collected traveling-wave data. (b) shows a plot of the uv coordinates retrieved for vertices on the discrete triangle mesh representation of the V1 visual area. (c) shows a cut region from the V1 shown in (a) with smooth gradient color. (d) is the resulting mesh after conversion of the vertices coordinates to the parameterized coordinates while maintaining the topology.

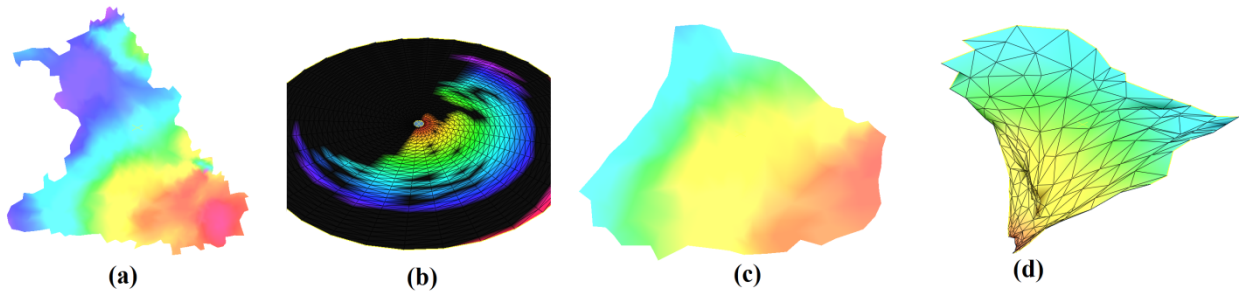

Figure 3. Parameterized coordinates comparison. (a) shows visual area V1 after slicing from left hemisphere of cortical mesh based on given outline of V1. (b) shows the plot of the parameterized coordinates for the conformally flattened V1 shown in (a). (c) shows a region cut from (a) that visually relatively smooth. (d) is the topological mesh generated from the parameterized coordinates of (c).

Finally, we compared cut V1 and V2 meshes with their parameterized coordinate counterpart versions by comparing their Beltrami coefficients. The Beltrami coefficients measure the local distortion of the mapping so that we get a quantitative description about how the mapping is close to being conformal.

In summary, the main contributions of the current work are as follows: First we introduce a novel quantitative way to measure the conformality of the brain visual field mapping. The method is based on our prior work on brain conformal mapping[21,22,23]. The method is mathematically rigorous and numerically stable. The results are intuitive and can quantify the human retinotopic mapping. Second, we developed a practical system that measures the mapping conformality by checking the histogram of the computed Beltrami coefficients. These tools may advance the area of research. Third, we apply our work to human brain visual mapping data and our results demonstrate some significant local conformality. Our results may lay down some theoretic foundation and provide practical experience for further investigation on human retinotopic mapping research.

The organization for this paper is as follows. Section 2 discusses the theory and methods used in this paper in more detail. Section 3 presents the experimental results. Section 4 concludes and gives final remarks.

2. CONFORMAL FLATTENING, PARAMETERIZED COORDINATES, AND BELTRAMI COEFFICIENT

2.1 Conformal flattening

We flattened the cortical mesh containing the visual regions using the spherical conformal method. Our algorithm follows the method described in Wang et. al.[21] with additional steps to back track and retry at specific points when convergence fails. It is known from computational conformal geometry that any closed genus zero surface can be conformally mapped to the sphere. This algorithm iteratively solves the nonlinear heat equation for the discrete case,

$$\frac{df(t)}{dt} = -\Delta f(t)$$

where f is a function defined on the genus zero surface and Δ is the Laplace operator. The heat equation is solved using the steepest descent method. The solution obtained by this method forms a möbius group and therefore requires an additional zero mass-center constraint in order to guarantee uniqueness. For each step of the algorithm, the vertices are moved along the geodesics of the sphere until the energy is minimized. The following equation describes the updating of the vertices coordinates at each step,

$$\Delta f(v) = f(v) - \delta t \times \Delta f^{\parallel}$$

where δt is the step size. Additionally, this equation requires the computation of the normal component

$$\Delta f^{\perp} = < \Delta f, f > f$$

and the tangential component

$$\Delta f^{\parallel} = \Delta f - \Delta f^{\perp}$$

of the discrete Laplacian. The proper selection of the step size, δt, is crucial in order for the algorithm to converge.

2.2 Recovering parameterized coordinates

We recovered the parameterized coordinates using the color map data that was selected and setup during the traveling-wave data collection phase. The gradient color map contains 256 colors spread across all the eccentricity and polar angle values used during data collection.[4,5,19] For each set of vertices within a cut visual area, we retrieve the associated eccentricity and polar angle color data value and compute the parameterized u and v coordinates as u = rcos(θ) and v = rsin(θ). Figure 4 shows how the gradient color map for eccentricity and polar angle translate to r and θ for computing the parameterized uv coordinates.

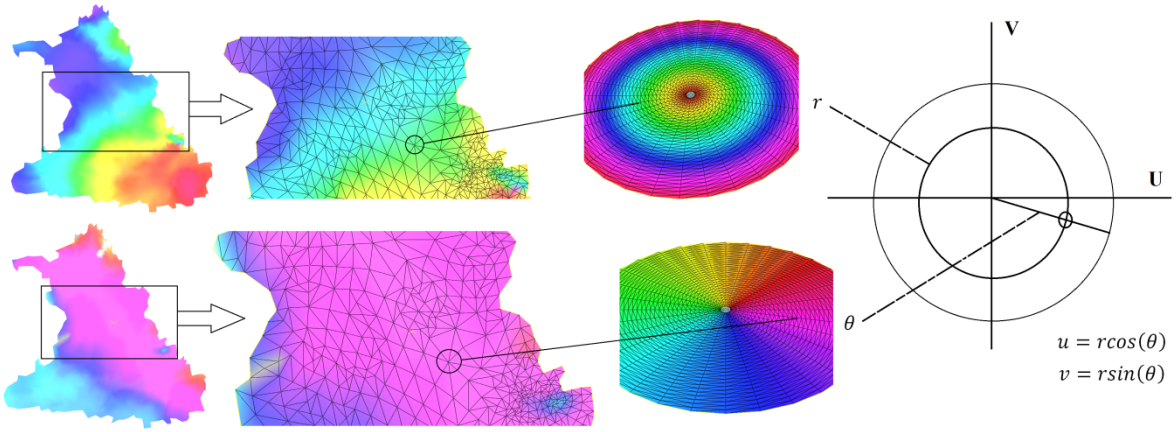

Figure 4. Recovering parameterized u and v coordinates from the vertices inside V1.

2.3 Beltrami coefficient

The Beltrami coefficient μ in Beltrami's equation

$$\frac{\partial f}{\partial \bar{z}} = \mu \frac{\partial f}{\partial z}$$

is a complex valued number

$$\mu = x + iy$$

that can be used to measure the the local conformality of the mapping between two surfaces. To compute the Beltrami coefficient, we write in complex form

$$\frac{\partial f}{\partial \bar{z}} = \frac{\partial f}{\partial x} + i\frac{\partial f}{\partial y}$$

$$\frac{\partial f}{\partial z} = \frac{\partial f}{\partial x} - i\frac{\partial f}{\partial y}$$

Since

$$f = u + iv$$

and

$$u = u(x, y)$$

$$v = v(x, y)$$

we can rewrite the complex form as

$$\frac{\partial f}{\partial \bar{z}} = \frac{\partial u}{\partial x} + i\frac{\partial v}{\partial x} + i\frac{\partial u}{\partial y} - \frac{\partial v}{\partial y}$$

$$\frac{\partial f}{\partial z} = \frac{\partial u}{\partial x} - i\frac{\partial v}{\partial x} - i\frac{\partial u}{\partial y} + \frac{\partial v}{\partial y}$$

All the values needed for computing the equations above can be obtained from the Jacobian matrix,

$$J = \begin{bmatrix} \frac{\partial u}{\partial x} & \frac{\partial u}{\partial y} \\ \frac{\partial v}{\partial x} & \frac{\partial v}{\partial y} \end{bmatrix}$$

of the mesh. The mapping is conformal when the value of both the real part x and imaginary part y is zero.

In practice, smooth surfaces are approximated by triangle meshes. Suppose $\emptyset: S_1 \to S_2$ is a map from the surface S_1 to the surface S_2. The map $\emptyset$ is approximated by a simplicial map, which maps vertices to vertices, edges to edges, and faces to faces. The derivative map $d\emptyset$ is approximated by the linear map from one face $[v_1, v_2, v_3]$ to another one $[w_1, w_2, w_3]$. First, we isometrically embed the triangle $[v_1, v_2, v_3]$, $[w_1, w_2, w_3]$ onto the plane $\mathbb{R}^2$; the planar coordinates of the vertices of v_i, w_j are denoted using the same symbols v_i, w_j. Then we explicitly compute the linear matrix for the derivative map $d\emptyset$,

$$d\emptyset = [w_3 - w_1, w_2 - w_1][v_3 - v_1, v_2 - v_1]^{-1}$$

With the derivative map, we can compute $\frac{\partial f}{\partial x}$ and $\frac{\partial f}{\partial y}$ so that we can use Beltrami's equation from above to compute μ. Further, we plot the histogram of the real and imaginary parts of the Beltrami coefficient to see how close they are to zero for analysis.

3. EXPERIMENTAL RESULTS AND DISCUSSION

Our analysis of the Beltrami coefficient shows that selected regions of V1 and V2 that contain reasonably smooth eccentricity and polar angle gradients do show significant local conformality. The selected region has to have smooth color gradient for both the eccentricity data and the polar angle data to yield good results. Finding such regions within a visual area is a dual optimization problem. Computation of the mean Beltrami coefficient for the entire V1 region of the right hemisphere yielded 0.1792 (real) and 0.0839 (imaginary) while the smoother gradient region yielded -0.0062 (real) and -0.0093 (imaginary). The reliable region is therefore more conformal than the whole V1 region in this case. Selection of a smooth region on the left hemisphere also resulted in getting the mean of the real part of the Beltrami coefficient to get closer to zero from 0.2219 down to 0.1584. The results are summarized in table 1.

Table 1. Beltrami coefficient V1 (Subject A)

Visual area	Beltrami coefficient part	Mean Beltrami coefficient	Vertices count
Left V1	Real	0.2219	1111
Left V1	Imaginary	0.0207	1111
Right V1	Real	0.1792	1490
Right V1	Imaginary	0.0839	1490

Table 2. Beltrami coefficient V1 for reliable region (Subject A)

Visual Area	Beltrami coefficient part	Mean Beltrami coefficient	Vertices count
Left V1	Real	0.1584	85
Left V1	Imaginary	0.0410	85
Right V1	Real	-0.0062	73
Right V1	Imaginary	-0.0093	73

The dual optimization problem of finding a region within the visual areas where the color gradient is smooth by observation is a difficult manual step that can benefit from the usage of an algorithmic tool. Figures 5 to 7 illustrates the

steps for extracting the smooth gradient color region from V1 and generating the resulting parameterized uv mesh for the right hemisphere. First, figure 5 shows the selected smooth gradient color region within the V1 region. Next, figure 6 shows the selected smooth gradient color region cut from the V1 region in figure 5. Notice how the color gradient is smooth for the eccentricity color data (left) and polar angle color data (right). Last, figure 7 shows the resulting topological mesh obtained after computing the uv coordinates of vertices inside the smooth region. Visually, most of the angles can be observed to have been preserved through the transformation and confirms the Beltrami coefficient results above. Similarly figures 8 and 9 shows the selected smooth gradient color region and the parameterized uv mesh result for the left hemisphere.

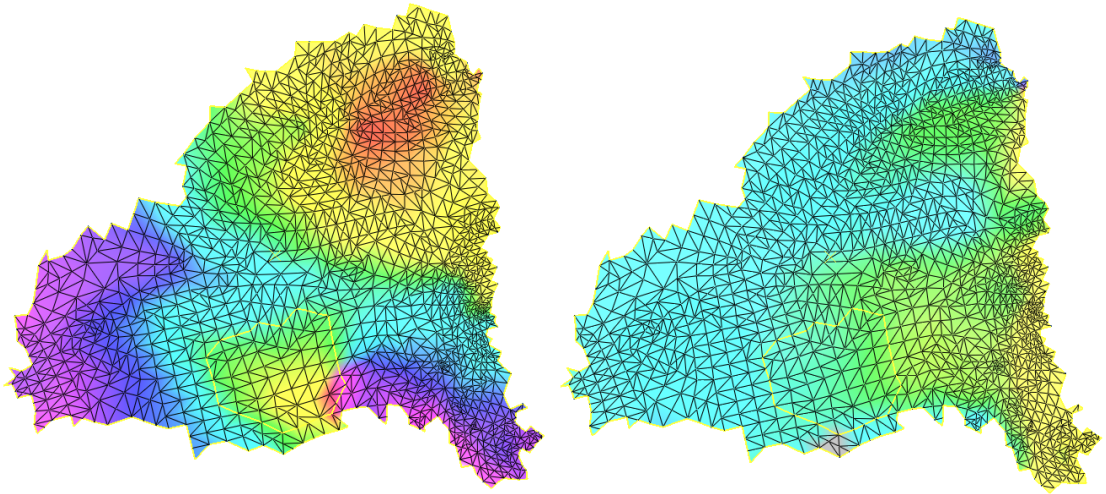

Figure 5. Right hemisphere V1 (Subject A) eccentricity (left) and polar angle (right) conformal flattened meshes. The yellow edges trace the boundary for a region that has visually smooth gradient.

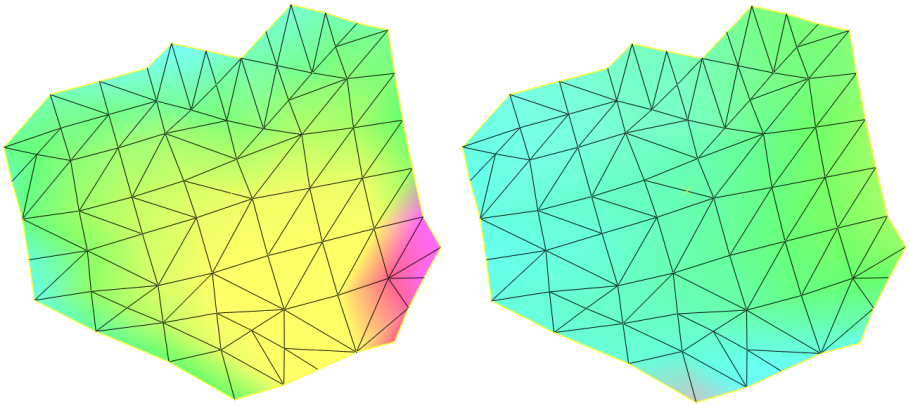

Figure 6. Right hemisphere V1 (Subject A) reliable region. Eccentricity (left) color map applied to vertices. Polar angle (right) color map applied to vertices.

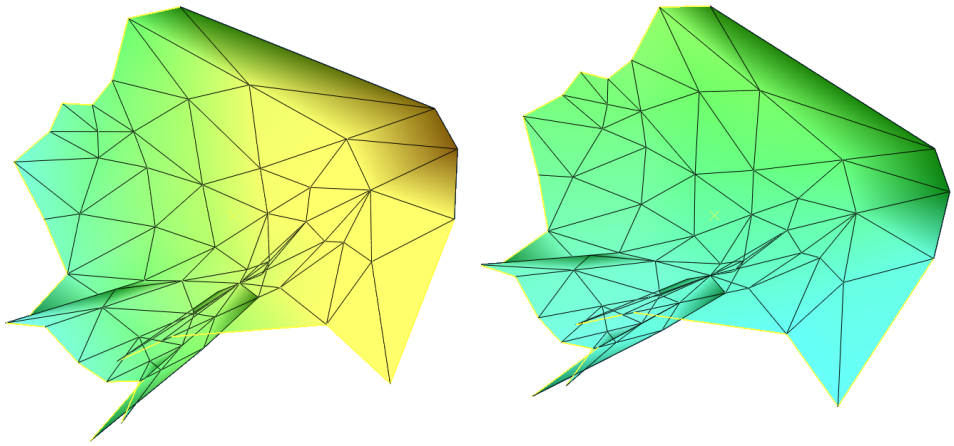

Figure 7. Right hemisphere V1 (Subject A) reliable region recovered parameterized mesh with eccentricity and polar angle gradient color map applied for visualization. Eccentricity (left) color map applied to vertices. Polar angle (right) color map applied to vertices.

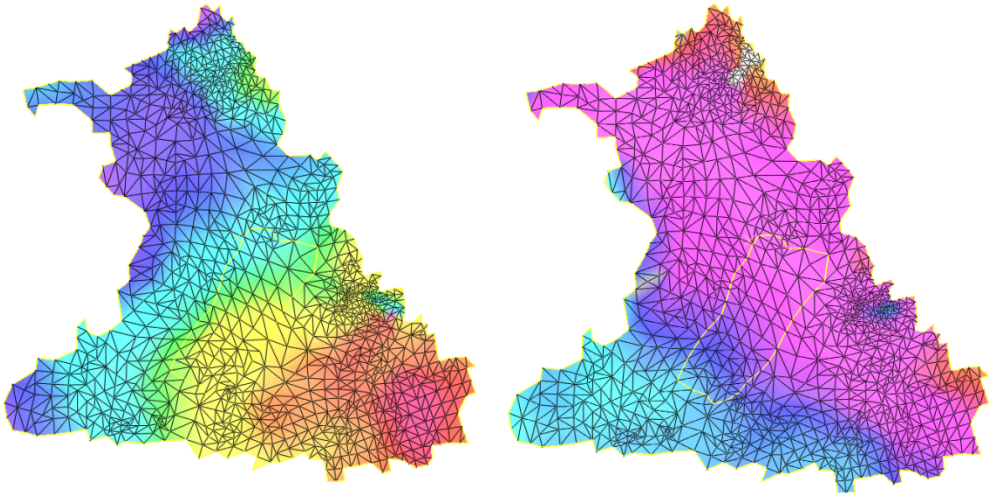

Figure 8. Left hemisphere V1 (Subject A) eccentricity (left) and polar angle (right) conformal flattened meshes. The yellow edges trace the boundary for a region that has visually smooth gradient.

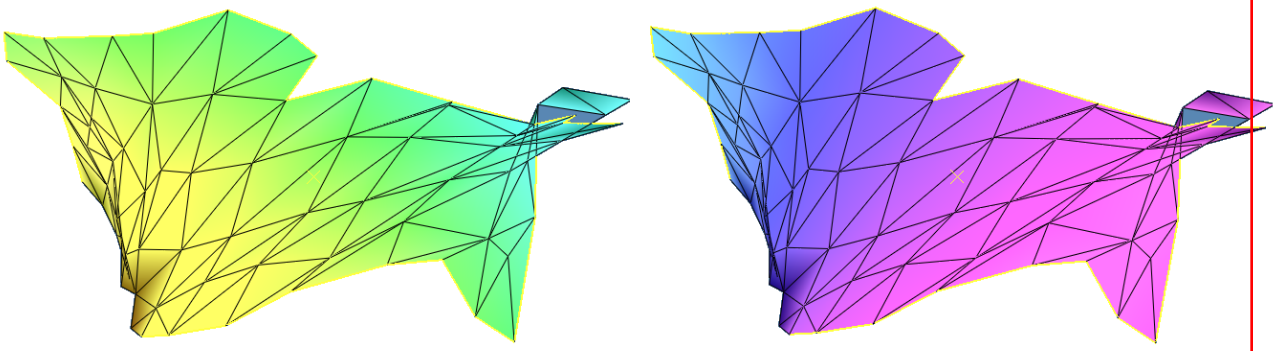

Figure 9. Left hemisphere V1 (Subject A) reliable region recovered parameterized mesh with eccentricity and polar angle gradient color map applied for visualization. Eccentricity (left) color map applied to vertices. Polar angle (right) color map applied to vertices.

4. CONCLUSION

These early results suggest that V1 and V2 exhibit local conformality and warrant further investigation of this approach for analysis of early and higher visual cortex. By computing the mean Beltrami coefficient on selected regions with smooth gradient color data, we have demonstrated that these regions are locally conformal. This result provides a new way to study and analyze retinotopic mappings. To consistently find good regions, there needs to be an automatic and algorithmic way to solve the dual optimization problem of finding smooth gradient color for eccentricity and polar angle. Although there are challenges that still need to be overcome, these preliminary results are encouraging and suggest that a mathematical model based on conformal geometry and Beltrami coefficient can be used to characterize the early VFMs in human visual cortex. In the future, we look to further explore using this method on more data sets and study the distribution of the mean Beltrami coefficient across the data sets.

REFERENCES

[1] Balasubramanian, M., J. Polimeni and E. L. Schwartz, "The V1 -V2-V3 complex: quasiconformal dipole maps in primate striate and extra-striate cortex", Neural Netw 15, 1157-1163 (2002).
[2] Balasubramanian, M., J. R. Polimeni and E. L. Schwartz, "Near-isometric flattening of brain surfaces", Neuroimage 51, 2, 694-703 (2010).
[3] B. Barton, J. H. Venezia, K. Saberi, G. Hickok, and A. A. Brewer. Orthogonal acoustic dimensions define auditory field maps in human cortex. Proc. Natl. Acad. Sci. U.S.A., 109(50):20738–20743, Dec 2012.
[4] A. A. Brewer. Visual maps: To merge or not to merge. Curr. Biol., 19(20):R945–947, Nov 2009.
[5] A. A. Brewer, J. Liu, A. R. Wade, and B. A. Wandell. Visual field maps and stimulus selectivity in human ventral occipital cortex. Nat. Neurosci., 8:1102–1109, Aug 2005.
[6] DeYoe EA, Carman GJ, Bandettini P, Glickman S, Wieser J, Cox R, Miller D, Neitz J. (1996): Mapping striate and extrastriate visual areas in human cerebral cortex. Proc Natl Acad Sci U S A 93(6):2382-6.
[7] Duncan RO, Boynton GM. (2003): Cortical magnification within human primary visual cortex correlates with acuity thresholds. Neuron 38(4):659-71.
[8] Engel SA, Glover GH, Wandell BA. (1997): Retinotopic organization in human visual cortex and the spatial precision of functional MRI. Cereb Cortex 7(2):181-92.
[9] Engel SA, Rumelhart DE, Wandell BA, Lee AT, Glover GH, Chichilnisky EJ, Shadlen MN. (1994): fMRI of human visual cortex. Nature 369(6481):525.
[10] Hansen, K. A., S. V. David and J. L. Gallant, "Parametric reverse correlation reveals spatial linearity of retinotopic human V1 BOLD response", Neuroimage 23, 233-241 (2004).
[11] Polimeni, J. R., M. Balasubramanian and E. L. Schwartz, "Multi-area visuotopic map complexes in macaque striate and extra-striate cortex", Vision Res. 46, 3336-3359 (2006).
[12] Qiu, A., B. J. Rosenau, A. S. Greenberg, M. K. Hurdal, P. Barta, S. Yantis and M. I. Miller, “Estimating linear cortical magnification in human primary visual cortex via dynamic programming”, Neuroimage 31, 1, 125-138 (2006).
[13] Schneider W, Noll DC, Cohen JD. (1993): Functional topographic mapping of the cortical ribbon in human vision with conventional MRI scanners. Nature 365(6442):150-3.
[14] Schwartz EL. (1977): The development of specific visual connections in the monkey and the goldfish: outline of a geometric theory of receptotopic structure. J Theor Biol 69(4):655-83.
[15] Schwartz, E. L., "Cortical mapping and perceptual invariance: a reply to Cavanagh", Vision Res. 23, 831-835 (1983).
[16] Sereno MI, Dale AM, Reppas JB, Kwong KK, Belliveau JW, Brady TJ, Rosen BR, Tootell RB. (1995): Borders of multiple visual areas in humans revealed by functional magnetic resonance imaging. Science 268(5212):889-93.
[17] Tootell RB, Reppas JB, Kwong KK, Malach R, Born RT, Brady TJ, Rosen BR, Belliveau JW. (1995): Functional analysis of human MT and related visual cortical areas using magnetic resonance imaging. J Neurosci 15(4):3215-30.
[18] Vanni, S., L. Henriksson and A. C. James, "Multifocal fMRI mapping of visual cortical areas", Neuroimage 27, 95-105 (2005).
[19] B. A.Wandell, A. A. Brewer, and R. F. Dougherty. Visual field map clusters in human cortex. Philos. Trans. R. Soc. Lond., B, Biol. Sci., 360:693–707, Apr 2005.

[20] Wandell BA, Winawer J. (2011): Imaging retinotopic maps in the human brain. Vision Res 51(7):718-37.
[21] Wang Y, Gu X, Chan TF, Thompson PM, Yau S-T. 2004. Intrinsic Brain Surface Conformal Mapping using a Variational Method. Proc. SPIE: SPIE. p 241--252.
[22] Wang Y, Lui LM, Gu X, Hayashi KM, Chan TF, Toga AW, Thompson PM, Yau S-T. (2007): Brain Surface Conformal Parameterization using Riemann Surface Structure. IEEE Trans. Med. Imag. 26(6):853-865.
[23] Wang Y, Shi J, Yin X, Gu X, Chan TF, Yau S-T, Toga AW, Thompson PM. (2011): Brain Surface Conformal Parameterization with the Ricci Flow. IEEE Trans. Med. Imag. (In Press).